# Simple Explanation for the Observed Power Law Distribution of Line Intensity in Complex Many-Electron Atoms

Keisuke Fujii[1,2,*] and Julian C. Berengut[3,2]

[1]Department of Mechanical Engineering and Science, Graduate School of Engineering, Kyoto University, Kyoto 615-8540, Japan

[2]Max-Planck-Institut für Kernphysik, Saupfercheckweg 1, 69117 Heidelberg, Germany

[3]School of Physics, University of New South Wales, New South Wales 2052, Australia

(Received 22 October 2019; revised manuscript received 30 January 2020; accepted 13 April 2020; published 7 May 2020)

It has long been observed that the number of weak lines from many-electron atoms follows a power law distribution of intensity. While computer simulations have reproduced this dependence, its origin has not yet been clarified. Here we report that the combination of two statistical models—an exponential increase in the level density of many-electron atoms and local thermal equilibrium of the excited state population—produces a surprisingly simple analytical explanation for this power law dependence. We find that the exponent of the power law is proportional to the electron temperature. This dependence may provide a useful diagnostic tool to extract the temperature of plasmas of complex atoms without the need to assign lines.

DOI: 10.1103/PhysRevLett.124.185002

It has long been known that the number of weak lines emitted by many-electron atoms in plasmas follows an intensity power law. In 1982 Learner pointed out this law for the first time when measuring emission lines from a hollow cathode lamp containing iron atoms [1]. He observed that the number density of lines with a given intensity $I$, $\rho_I(I)$, exhibits a power law dependence on $I$ [2],

$$\rho_I(I) \propto I^{-1.50}. \tag{1}$$

He also reported that $\rho_I(I)$ in different wavelength regions all follow this power law with the same exponent, indicating an ergodic property of the emission line distribution [1].

This work has stimulated much discussion. A theoretical study by Scheeline showed that this power law does not hold for hydrogen atom spectra [3]. In contrast, the emission spectrum from arsenic, which has a much more complex electronic structure than hydrogen, shows an intensity distribution closer to the power law, but with a different value of the exponent [4]. Bauche-Arnoult and Bauche reported a simulation with a collisional-radiative model for a neutral iron atom and demonstrated that the power law dependence is again reproduced [5]. Their exponent was 17%–25% smaller than the Learner's value, but the reason was not clarified.



Pain recently reviewed this power law dependence problem and presented a discussion regarding fractal dimension and quantum chaos [6]. According to his discussion, the line strength distribution evaluated under the fully quantum-chaos assumption does not explain Learner's law. As presented in his review [6], as well as in the book [7], the origin of this power law is still not understood, despite almost 40 years passing since the first report.

In this Letter, we present a surprisingly simple explanation of Learner's law. We assume local thermal equilibrium of the excited state population and an exponential increase in the level density of complex atoms, which has been reported in several many-electron atoms and ions (e.g., [8,9]). Combining these, we show below that the number of levels with a given population follows a power law distribution. An assumption of independently and identically distributed radiative transition rates then directly gives Learner's law in the form

$$\rho_I(I) \propto I^{-2kT_e/\epsilon_0-1}, \tag{2}$$

where $k$ is Boltzmann's constant and $T_e$ is the electron temperature in the plasma. $\epsilon_0$ is a scale parameter representing the level density growth rate against the excited energy [see Eq. (3) for its definition], which can be estimated either from the experimentally derived energy levels or from *ab initio* atomic structure calculations [9].

Plasma spectroscopy has been developed from simpler systems, e.g., hydrogen and rare gas atoms. It is known that comparison between intensity ratios of certain emission lines and collisional-radiative models provides us with information about plasma parameters, such as electron

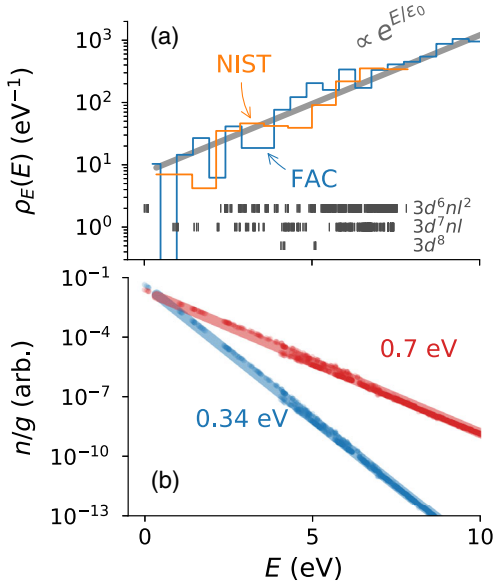


FIG. 1. (a) State density of neutral iron against excitation energy. The orange histogram is computed from the measurement data compiled in NIST ASD [21]. The measured energy levels (846 entries) are shown by the vertical bars in the figure. The blue histogram shows the state density computed from the FAC [22]. The gray line is an exponential dependence, Eq. (3), with $\epsilon_0 = 1.97$ eV, which fits both densities well. (b) Population distribution computed using collisional-radiative modeling with $T_e = 0.34$ eV (blue points) and 0.7 eV (red points) and electron density $n_e = 10^{20}$ m$^{-3}$. The blue and red bold lines present the Boltzmann distribution [Eq. (4)] with effective temperatures 0.32 and 0.61 eV, respectively.

temperature and density [10–13]. This requires correct line identifications and accurate atomic data, such as energy levels, oscillator strengths, and collision cross sections. However, accurate atomic data for open-shell atoms is difficult to obtain despite numerous demands for plasma diagnostics with complex atoms, ranging from laser produced plasmas for extreme-ultraviolet light sources [14–16] and heavy-metal-contaminated fusion plasmas [17,18] to the emissions found after the $r$-process supernova (kilonova) [19,20]. Our result, Eq. (2), suggests an advantage of using intensity statistics for diagnosing plasmas with many-electron atoms, where accurate *ab initio* simulations of such complex spectra are still difficult with currently available theory and computers.

Next we derive Eq. (2), illustrating our assumptions using Learner's example of neutral iron. Figure 1(a) shows the level density of neutral iron $\rho_E(E)$, the number of levels with given excited energy $E$. This state density is evaluated from the measured energy levels taken from the Atomic Spectral Database (ASD) by the National Institute of Standards and Technology (NIST) [21]. The observed energy levels are shown by the vertical bars in the figure.

It is well known that the excited level density in the quantum many-body system increases nearly exponentially. One simple but common approximation is [9,23,24]

$$\rho_E(E) \propto \exp\left(\frac{E}{\epsilon_0}\right), \tag{3}$$

where $\epsilon_0$ is an atom-specific energy scale, which depends on the number of active electrons and the number, degeneracy, and distribution of single particle states in the atom [9]. It can be calculated numerically, derived from experimental energy levels, or estimated using combinatorics. Dzuba and Flambaum presented that for open-$d$- or $f$-shell atoms the state density follows Eq. (3), at least below the ionization energy [9]. For neutral iron, we find Eq. (3) well represents the level density with $\epsilon_0 \approx 1.97 \pm 0.04$ eV, as indicated by the solid line in Fig. 1(a). Note that this value is obtained by the maximum-likelihood estimation of the simulated energy levels.

Let us assume local thermal equilibrium for the excited state population. The population in state $i$ with energy $E_i$ is given as

$$n_i \propto g_i \exp\left(-\frac{E_i}{kT_e}\right), \tag{4}$$

where $g_i$ is the statistical weight of the state $i$ ($g_i = 2J_i + 1$, where $J_i$ is the total angular momentum quantum number of state $i$). This equilibrium is valid in plasmas with high electron density and low electron temperature [11]. By substituting Eq. (3) into Eq. (4), the number of states having the population $n \sim n + dn$ can be written as

$$\rho_n(n)dn = \rho_E(E)dE \propto \frac{1}{n}\rho_E(E)dn \tag{5}$$

$$\propto \frac{1}{n}\exp\left(-\frac{kT_e}{\epsilon_0}\log n\right)dn \tag{6}$$

$$\propto n^{-kT_e/\epsilon_0 - 1}dn, \tag{7}$$

where $dE$ is the energy interval corresponding to $dn$, the relation of which can be obtained from Eq. (4). We assume in Eq. (6) that the statistical weight is distributed uniformly over the energy and therefore we omit it from the equation. This power law originates from the combination of one exponentially increasing variable and another exponentially decreasing variable. This is a typical mathematical structure responsible for the emergence of power laws [25].

The emission intensity $I_{ij}$ corresponding to the transition $i \to j$, where $j$ is the lower state, is proportional to the upper state population $n_i$, the transition energy cubed $\omega_{ij}^3 = (E_i - E_j)^3$, and the line strength $S_{ij}$ between $i$ and $j$ states. In many-electron atoms with sufficient basis-state mixing, i.e., in quantum-chaotic systems, the probability distribution of $S_{ij}$ can be well approximated as uniform and independent and can be modeled using the Porter-Thomas distribution $p(S) \propto (1/\sqrt{2\pi S_0 S})\exp(-S/2S_0)$, with a constant $S_0$ [8,26–29]. This approximation is obtained by

modeling the Hamiltonian with a Gaussian orthogonal ensemble. As this distribution decays considerably faster than the power law in the large $S$ limit, we can safely approximate that $S_{ij}$ is a constant for all pairs of levels. Therefore, the intensity $I_{ij}$ is approximated as

$$I_{ij} \propto \omega_{ij}^3 S_0 n_i. \tag{8}$$

A more detailed and precise discussion can be found in the Supplemental Material [30].

The number of emission lines from state $i$ observed in photon energy range $\omega \sim \omega + d\omega$ is proportional to the number of levels in this energy range, $\rho_E(E_i - \omega)d\omega$. By considering the number of emission lines with a given intensity range $I \sim I + dI$, we arrive at Eq. (2),

$$\rho_I(I)dI = \int_\Omega \rho_E(E-\omega)\rho_E(E)d\omega dE \propto I^{-2kT_e/\epsilon_0 - 1}dI,$$

where the integration along $\omega$ is taken over the observed photon energy range $\Omega$. Here the variable $E$ is changed to $I$ based on Eqs. (4) and (8). The factor 2 newly appears in the exponent of $I$ compared with Eq. (7).

The exponent in Eq. (2) does not depend on $\Omega$. This is consistent with Learner's observation that the emission line density in different wavelength regions all show the power law dependence with the same exponent [1]. Learner suggested a relation between the exponent and a constant, $\log_{10}\sqrt{2}$ [1]. In contrast, our Letter clearly indicates a relation with $T_e$ and the atom-specific constant $\epsilon_0$.

By comparing the exponents in Eqs. (1) and (2), $T_e$ in Learner's experiment is estimated as $(1.50-1)\epsilon_0/2 \approx 0.49$ eV. Although in Ref. [5] it is claimed that $T_e$ higher than 0.34 eV is not realistic, $T_e$ in hollow cathode discharges reported in literature varies from 0.2 to 3 eV depending on the cathode element, filler gas pressure, and discharge current [38,39]. Therefore, 0.49 eV may not be a surprising value for $T_e$ in a hollow cathode discharge.

Bauche-Arnoult and Bauche have used $T_e = 0.34$ eV for their simulation [5], which is smaller than 0.49 eV. They obtained $-1.392 \pm 0.017$ for the exponent [40], which is consistently smaller in magnitude than Learner's value. Our above discussion further provides an explanation for one argument in their paper, i.e., the higher the electron temperature, the larger the magnitude of the exponent [5].

We carry out an *ab initio* simulation of the emission spectrum of neutral iron with the flexible atomic code (FAC) [22]. The FAC uses the relativistic Hartree-Fock method to calculate the electronic orbitals and configuration interaction to approximate the electron-electron interaction. The excited state population and the emission line intensity are evaluated by the collisional-radiative model implemented in the FAC, where the steady state of population in the plasma is assumed. For the collisional-radiative calculation we consider spontaneous emission, electron-impact excitation, deexcitation, and ionization, as well as autoionization of levels above the ionization threshold, as elementary processes in plasmas. These rates are also calculated by the FAC.

We assume $T_e = 0.34$ eV and the electron density $n_e = 10^{20}$ m$^{-3}$, similar to Bauche-Arnoult and Bauche [5]. We also perform the simulation with $T_e = 0.70$ eV to observe the $T_e$ dependence of the exponent. Note that in the FAC computations we do not explicitly adopt either of our two assumptions, namely, the exponential increase of the state density and the local thermal equilibrium of the population.

The state density of a neutral iron atom computed by the FAC is shown in Fig. 1(a) by a blue histogram. It shows a similar exponential dependence to the measured data, NIST ASD. Figure 1(b) shows the excited state population computed by the FAC. Although we do not assume local thermal equilibrium, the population follows the exponential function. The exponents for $T_e = 0.34$ and 0.70 eV cases are estimated by the least-squares method to be 0.32 and 0.61 eV, respectively, which are similar to the electron temperature. Note that the slight difference between $T_e$ and the exponent in the population is caused by a small violation of the local thermal equilibrium in plasma [11]. Based on approximate electron-impact excitation and deexcitation rates, we find that this effective temperature has a weak $n_e$ dependence and approaches $T_e$ in the large $n_e$ limit. Even with a smaller electron density, $n_e = 10^{17}$ m$^{-3}$, this temperature is expected to be $\approx 0.7T_e$ for the $T_e = 0.34$ eV case. Details can be found in the Supplemental Material [30].

The histograms in Fig. 2(a) show the state density $\rho_n(n)$ with given population $n$ (but scaled by $n$ to aid visualization). The solid blue and red lines are computed according to Eq. (7) with $T_e = 0.32$ and 0.61 eV, respectively [the same temperatures used in Fig. 1(b)]. Their agreement is clear.

Figure 2(b) shows the line intensity distribution $\rho_I(I)$ in the visible and infrared wavelength range (scaled by $I$ for visualization). The solid lines show Eq. (2) with $T_e = 0.32$ and 0.61 eV for the two cases. This also agrees with the above discussion, particularly in the first three orders studied by Learner.

In Eq. (2), we show that the exponent exclusively depends on $T_e$ and $\epsilon_0$, but not on other atomic data, such as level energies, transition rates, and collision cross sections. The only value we require, $\epsilon_0$, is known to be accurately calculated with several atomic structure packages [9]. Therefore, Eq. (2) may be useful as a quick diagnostic method for many-electron atom plasmas.

As Eq. (2) is scale free for $I$, the power law dependence is not affected by the system's sensitivity (see the Supplemental Material for details [30]). Thus, no system calibration is required for estimation of $T_e$. We only need to know the dominant (in terms of the number of emission lines) atom in the plasma.

We have applied this approach to the emission spectra measured for thorium plasmas. Figures 3(a) and 3(b) show spectra measured from a thorium-argon hollow cathode plasma with 75 [41] and 20 mA discharge current [42],

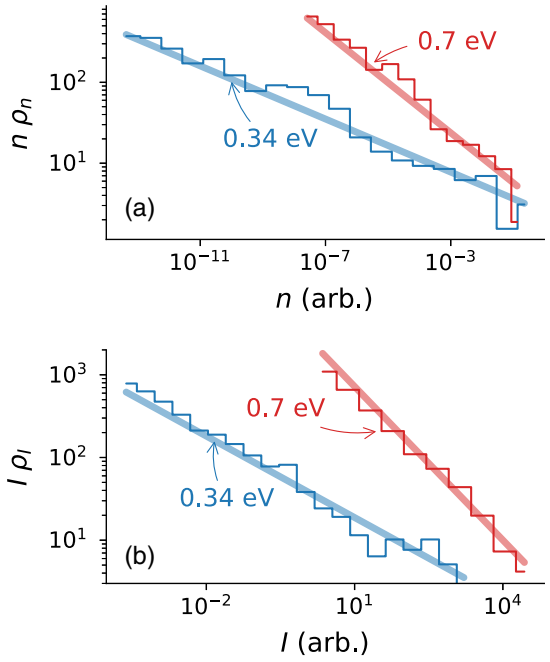


FIG. 2. (a) State density distribution $\rho_n(n)$, multiplied by $n$ to aid visualization. The blue histogram presents the computed result with $T_e = 0.34$ eV, while red presents the result with $T_e = 0.7$ eV. Both distributions follow the power law. (b) Density distribution of emission lines $\rho_I(I)$, computed by the FAC. Again, the vertical values are multiplied by $I$ to aid visualization. The bold lines in (a) and (b) are not fit results but theoretical models [Eqs. (7) and (2), respectively] with the same electron temperatures used in Fig. 1(b).

respectively, with a 1-m Fourier transform spectrometer. The original data can be downloaded from the Kitt Peak National Observatory website [43]. Only the spectra in the 510–560 nm wavelength range are shown and analyzed in this Letter. Dots in each panel show the line centers and peaks detected in the two spectra.

Although not all emission lines in these spectra have been identified, we assume that most of the lines are from neutral thorium. We compute $\rho_I(I)$ from all line intensities in the wavelength range [Fig. 3(c)]. The two histograms generated from the spectra show a power law distribution. $\rho_I(I)$ for the higher current discharge shows a steeper slope.

We estimate the exponent of these distributions using the maximum-likelihood method. The optimized distributions are shown by solid lines (and their 2-$\sigma$ uncertainty by colored bands) in Fig. 3(c). They fit both histograms. Estimated values of the exponent are $1.71 \pm 0.03$ and $1.64 \pm 0.03$ for the 75 and 20 mA disharges, respectively. From Eq. (2) and the value $\epsilon_0 \approx 0.68$ eV for neutral thorium by Dzuba and Flambaum [9], electron temperatures for these plasmas are estimated as $0.24 \pm 0.01$ and $0.21 \pm 0.01$ eV, respectively. A higher $T_e$ value is estimated for the higher current discharge. Although the positive current dependence of the temperature is not trivial [38], this dependence qualitatively supports our model. Because there are no radiative rates reported for neutral thorium, it is difficult to estimate $T_e$ for this plasma by conventional methods. To our knowledge, the above procedure is the only one available to estimate $T_e$ for thorium plasmas.

Although there are significant demands to diagnose plasmas with many-electron atoms, quantitative comparison with an *ab initio* computer simulation model is not yet accurate enough, because of the unavailability of accurate atomic data. Our result suggests a possibility of plasma diagnostics that requires only the energy level statistics and the emission intensity statistics. Although the validity of the local thermal equilibrium assumption should be investigated further, this may open the door to a new statistical plasma spectroscopy.

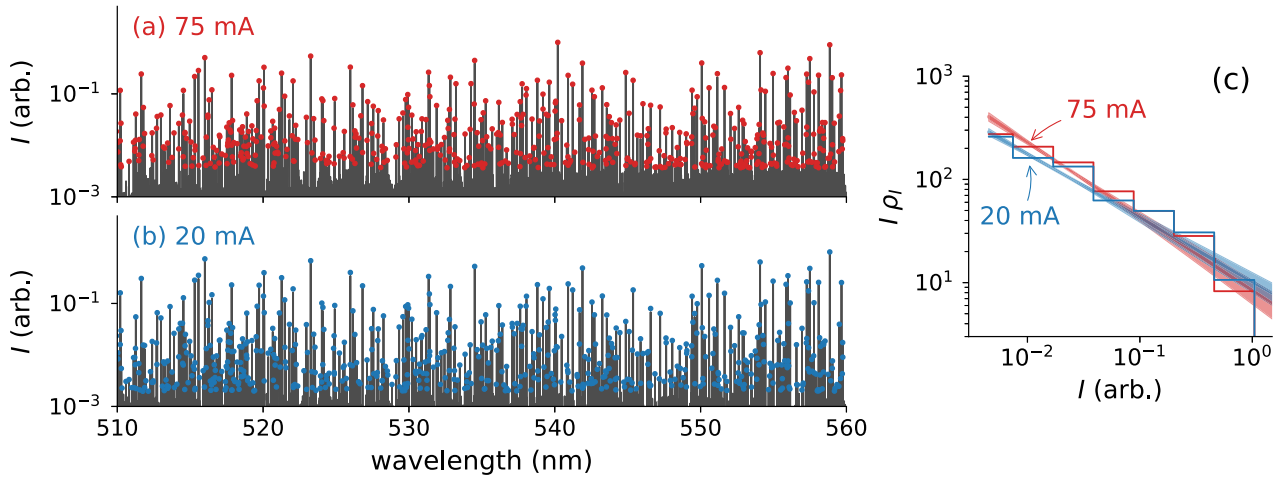


FIG. 3. Emission spectra observed from thorium-argon hollow cathode plasmas (a) with 75 mA discharge current [41] and (b) with 20 mA discharge current [42]. Dots indicate the centers and intensities of emission lines detected in each spectrum. (c) Intensity distributions computed from the spectra in (a) and (b). Straight lines show the optimized power law distribution by maximum-likelihood method. The exponents for the 75 and 20 mA discharges are $1.71 \pm 0.03$ and $1.64 \pm 0.03$, respectively.

In summary, we have presented a simple explanation of Learner's law, where the histogram of the emission line intensities from many-electron atoms follows a power law. We observed that the exponent is analytically represented with $T_e$ and $\epsilon_0$. A similar discussion should also be applicable to other fermionic many-body systems as long as the two assumptions are satisfied. Although as yet there are no reports about the emission statistics except for many-electron atoms, it is interesting to investigate other systems, such as heavy nuclei. This is left for future study.

This work was partly supported by JSPS KAKENHI Grant No. 19K14680, the grant of Joint Research by the National Institutes of Natural Sciences (NINS) (NINS Program No. 01111905), and partly by the Max-Planck Society for the Advancement of Science. J. C. B. is supported by the Alexander von Humboldt Foundation. We thank José Crespo López-Urrutia, Tomoyuki Obuchi, and Akira Nishio for useful discussions.

*fujii@me.kyoto-u.ac.jp

[1] R. C. M. Learner, J. Phys. B **15**, L891 (1982).
[2] Note that although he used a different base, two for the intensity and ten for the line number, we use $e$ as the base and present the converted value by $b \log 10/\log 2 - 1$ for later convenience, where $b$ is the original value, $-0.15$.
[3] A. Scheeline, Anal. Chem. **58**, 3103 (1986).
[4] A. Scheeline, Anal. Chem. **58**, 802 (1986).
[5] C. Bauche-Arnoult and J. Bauche, J. Quant. Spectrosc. Radiat. Transfer **58**, 441 (1997).
[6] J.-C. Pain, High Energy Density Phys. **9**, 392 (2013).
[7] J. Bauche, C. Bauche-Arnoult, and O. Peyrusse, *Atomic Properties in Hot Plasmas* (Springer International Publishing, Cham, 2015).
[8] V. V. Flambaum, A. A. Gribakina, and G. F. Gribakin, Phys. Rev. A **58**, 230 (1998).
[9] V. A. Dzuba and V. V. Flambaum, Phys. Rev. Lett. **104**, 213002 (2010).
[10] H. R. Griem, in *Fast Electrical and Optical Measurements* (Springer Netherlands, Dordrecht, 1986), pp. 885–910.
[11] T. Fujimoto, in *Plasma Polarization Spectroscopy* (Springer Berlin Heidelberg, Berlin, 2004), pp. 29–49, ISBN 978019 8530282.
[12] K. Sawada, K. Eriguchi, and T. Fujimoto, J. Appl. Phys. **73**, 8122 (1993).
[13] M. Goto, J. Quant. Spectrosc. Radiat. Transfer **76**, 331 (2003).
[14] N. Böwering, M. Martins, W. N. Partlo, and I. V. Fomenkov, J. Appl. Phys. **95**, 16 (2004).
[15] M. Masnavi, M. Nakajima, E. Hotta, K. Horioka, G. Niimi, and A. Sasaki, J. Appl. Phys. **101**, 033306 (2007).
[16] C. Suzuki, F. Koike, I. Murakami, N. Tamura, and S. Sudo, J. Phys. B **45**, 135002 (2012).
[17] T. Pütterich, R. Neu, R. Dux, A. D. Whiteford, and M. G. O'Mullane, Plasma Phys. Controlled Fusion **50**, 085016 (2008).
[18] I. Murakami, H. Sakaue, C. Suzuki, D. Kato, M. Goto, N. Tamura, S. Sudo, and S. Morita, Nucl. Fusion **55**, 093016 (2015).
[19] E. Pian *et al.*, Nature (London) **551**, 67 (2017).
[20] M. Tanaka, D. Kato, G. Gaigalas, P. Rynkun, L. Radžit, S. Wanajo, Y. Sekiguchi, N. Nakamura, H. Tanuma, I. Murakami, and H. A. Sakaue, Astrophys. J. **852**, 109 (2018).
[21] A. Kramida, Y. Ralchenko, J. Reader (NIST ASD Team) (2018), NIST Atomic Spectra Database (version 5.6.1), https://physics.nist.gov/asd, 2019.
[22] M. F. Gu, Can. J. Phys. **86**, 675 (2008).
[23] D. Ter Haar, Phys. Rev. **76**, 1525 (1949).
[24] T. Von Egidy, A. N. Behkami, and H. H. Schmidt, Nucl. Phys. **A454**, 109 (1986).
[25] M. V. Simkin and V. P. Roychowdhury, Phys. Rep. **502**, 1 (2011).
[26] C. E. Porter and R. G. Thomas, Phys. Rev. **104**, 483 (1956).
[27] S. M. Grimes, Phys. Rev. C **28**, 471 (1983).
[28] S. E. Bisson, E. F. Worden, J. G. Conway, B. Comaskey, J. A. D. Stockdale, and F. Nehring, J. Opt. Soc. Am. B **8**, 1545 (1991).
[29] V. V. Flambaum, A. A. Gribakina, G. F. Gribakin, and M. G. Kozlov, Phys. Rev. A **50**, 267 (1994).
[30] See Supplemental Material at http://link.aps.org/supplemental/10.1103/PhysRevLett.124.185002 for more detailed derivation of Eq. (2), as well as the validity condition of the local-thermal-equilibrium assumption, which includes Refs. [8,26–28,31–37].
[31] R. Mewe, Astron. Astrophys. **20**, 215 (1972).
[32] H. R. Griem, Phys. Rev. **131**, 1170 (1963).
[33] R. McWhirter, in *Plasma Diagnostic Techniques*, edited by R. Huddlestone and S. Leonard (Academic Press, New York, 1965), pp. 201–264.
[34] C. Suzuki, T. Higashiguchi, A. Sasanuma, G. Arai, Y. Fujii, Y. Kondo, T.-H. Dinh, F. Koike, I. Murakami, and G. O'Sullivan, Nucl. Instrum. Methods Phys. Res., Sect B **408**, 253 (2017).
[35] G. O'sullivan, B. Li, R. D 'arcy, P. Dunne, P. Hayden, D. Kilbane, T. Mccormack, H. Ohashi, F. O 'reilly, P. Sheridan, E. Sokell, C. Suzuki, and T. Higashiguchi, J. Phys. B **48**, 144025 (2015).
[36] H. Kawashima, K. Shimizu, T. Takizuka, K. Tobita, S. Nishio, S. Sakurai, and H. Takenaga, Nucl. Fusion **49**, 065007 (2009).
[37] A. Kukushkin, H. Pacher, V. Kotov, G. Pacher, and D. Reiter, Fusion Eng. Des. **86**, 2865 (2011).
[38] D. M. Mehs and T. M. Niemczyk, Appl. Spectrosc. **35**, 66 (1981).
[39] L. Meng, R. Raju, R. Flauta, H. Shin, D. N. Ruzic, and D. B. Hayden, J. Vacuum Sci. Technol. A **28**, 112 (2010).
[40] This value is also converted from the original value $b = -0.118 \pm 0.005$.
[41] B. Palmer and R. J. Engleman, Atlas of the thorium spectrum, Technical Report No. LA-9615, Los Alamos National Laboratory (LANL), Los Alamos, NM, 1980, https://www.osti.gov/biblio/6348879-atlas-thorium-spectrum.
[42] F. Kerber, G. Nave, and C. J. Sansonetti, Astrophys. J. Suppl. Ser. **178**, 374 (2008).
[43] Kitt Peak National Observatory Data Archives, ftp://nispdata.nso.edu, 2019.